The FEBS Journal

FEBS PRESS science publishing by scientists

SLC25A26 overexpression impairs cell function via mtDNA hypermethylation and rewiring of methyl metabolism

Alessio Menga[1], Erika M. Palmieri[2], Antonia Cianciulli[2], Vittoria Infantino[3], Massimiliano Mazzone[4], Antonio Scilimati[5], Ferdinando Palmieri[2], Alessandra Castegna[1,2] and Vito Iacobazzi[2]

1 National Cancer Research Center, Istituto Tumori 'Giovanni Paolo II', Bari, Italy
2 Department of Biosciences, Biotechnologies and Biopharmaceutics, University of Bari 'Aldo Moro', Italy
3 Department of Science, University of Basilicata, Potenza, Italy
4 Laboratory of Molecular Oncology and Angiogenesis, Department of Oncology, Vesalius Research Center, KU Leuven, Belgium
5 Department of Pharmacy, University of Bari 'Aldo Moro', Italy

Keywords
epigenetic mechanisms; methyl cycle; mtDNA methylation; *S*-adenosylmethionine; SLC25A26 mitochondrial carrier

Correspondence
A. Castegna, Department of Biosciences, Biotechnologies and Biopharmaceutics, University of Bari 'Aldo Moro', via Orabona 4, 70125 Bari, Italy
Fax: +39 080 5442770
Tel: +39 080 5442771
E-mail: alessandra.castegna@uniba.it
V. Iacobazzi, Department of Biosciences, Biotechnologies and Biopharmaceutics, University of Bari 'Aldo Moro', via Orabona 4, 70125 Bari, Italy
Fax: +39 080 5442770
Tel: +39 080 5442322
E-mail: vito.iacobazzi@uniba.it

(Received 15 August 2016, revised 1 December 2016, accepted 20 January 2017)

doi:10.1111/febs.14028

Cancer cells down-regulate different genes to give them a selective advantage in invasiveness and/or metastasis. The *SLC25A26* gene encodes the mitochondrial carrier that catalyzes the import of *S*-adenosylmethionine (SAM) into the mitochondrial matrix, required for mitochondrial methylation processes, and is down-regulated in cervical cancer cells. In this study we show that *SLC25A26* is down-regulated due to gene promoter hypermethylation, as a mechanism to promote cell survival and proliferation. Furthermore, overexpression of *SLC25A26* in CaSki cells increases mitochondrial SAM availability and promotes hypermethylation of mitochondrial DNA, leading to decreased expression of key respiratory complex subunits, reduction of mitochondrial ATP and release of cytochrome *c*. In addition, increased SAM transport into mitochondria leads to impairment of the methionine cycle with accumulation of homocysteine at the expense of glutathione, which is strongly reduced. All these events concur to arrest the cell cycle in the S phase, induce apoptosis and enhance chemosensitivity of SAM carrier-overexpressing CaSki cells to cisplatin.

Introduction

S-Adenosylmethionine (SAM) is the methyl donor fundamental for sustained epigenetic modifications, such as DNA methylation, and has been implicated in the pathogenesis underlying cancer development [1]. Abnormal DNA methylation patterns related to persistent infection of human papilloma virus (HPV) represent an early and frequent alteration in cervical carcinogenesis [2]. Indeed, several genes, such as those

Abbreviations
5-Aza, 5-aza-2′-deoxycytidine; CBS, cystathionine β-synthase; ChIP, chromatin immunoprecipitation; Cytb, cytochrome *b*; dC 2′-deoxycytidine; GSH, reduced glutathione; GSSG, oxidized glutathione; HPV, human papilloma virus; mdC, 5-methyl-2′-deoxycytidine; MeCP2, methyl CpG binding protein 2; mtDNA, mitochondrial DNA; ROS, reactive oxygen species; SAMC, *S*-adenosylmethionine carrier; SAM, *S*-adenosylmethionine.

for p16, death-associated protein kinase, tissue inhibitor of metalloproteinases-3 [3], E-cadherin [4,5], cell adhesion molecule 1 and T-cell differentiation protein [6,7], are down-regulated through DNA methylation, contributing to the development, progression and/or metastasis of cervical cancer. Identification of new gene targets of epigenetic regulation might be useful to shed light on the biological processes and the molecular basis of the development of cervical cancer.

SLC25A26 is the gene encoding *S*-adenosylmethionine carrier (SAMC), a member of the mitochondrial carrier family, a group of transport proteins that are found in the inner membrane of mitochondria [8,9]. The physiological role of SAMC is to catalyze the uptake of SAM, the universal methyl donor, from cytosol into mitochondria, where it is required for the methylation of DNA, RNA and proteins, and as an intermediate in the biosynthesis of lipoic acid and ubiquinone [10]. SAM is produced in the cytosol by the methionine cycle pathway, through the transfer of adenosine from ATP to methionine catalyzed by methionine adenosyltrasferase [11]. SAM transport into mitochondria strictly depends on its synthesis, which is known to be regulated by both cytosolic and mitochondrial metabolism [12]. Mitochondrial metabolism regulates production of SAM through synthesis of ATP and folate, the folate cycle reactions being duplicated in the cytosol and mitochondria. Furthermore, the methionine cycle is strictly related to the transsulfuration pathway, with homocysteine being the linking metabolite between synthesis of methionine and cysteine. Since cystathionine β-synthase (CBS), the enzyme producing cystathionine from homocysteine, is allosterically activated by SAM [13], glutathione production from cysteine is strictly related to the concentration of cytosolic SAM, which depends on the amount produced in the cytosol and withdrawn into the mitochondria. Similarly, availability of SAM to mitochondria might strongly modify the function of the mitochondrial targets of methylation. Mitochondrial DNA (mtDNA) is one of these targets. Methylation is known to modify mtDNA [14], leading to altered expression of mtDNA-encoded genes in normal and pathological conditions [15–17]. We have shown that methyl metabolism and SAM availability significantly influence the amount of mtDNA being methylated, suggesting that the flux through methyl metabolism and mitochondrial function might be tightly linked and reciprocally regulated [15]. Furthermore, Bellizzi *et al.* [18] have highlighted the importance of methylation of the regulatory region D-loop in regulating the expression of some mtDNA-encoded proteins (i.e. respiratory complex subunits) and tRNAs or ribosomal RNA, leading to altered mitochondrial functionality. Based on this evidence, the levels of *SLC25A26* expression are destined to have a strong impact on cell function by orchestrating several metabolic events. However, the conditions and the mechanisms by which *SLC25A26* expression is modulated are still elusive. Due to its relationship with the methyl metabolism, we hypothesized that *SLC25A26* could be a target gene for epigenetic modification in cervical cancer cells and this could have important consequences at both cellular and mitochondrial levels.

In this work we show for the first time that *SLC25A26* is down-regulated by an epigenetic mechanism in CaSki and HeLa cells, and we have investigated the biochemical and functional significance of its repression by evaluating the effects of its up-regulation on mtDNA methylation, mitochondrial oxidative phosphorylation, the methionine cycle and cell viability. This work also highlights the importance of mtDNA epigenetics and the complex metabolic and epigenetic mechanisms related to mtDNA methylation in regulating mitochondrial and cellular functions.

Results

SLC25A26 gene is down-regulated in CaSki cells by promoter hypermethylation

Both cervical cancer cell lines CaSki and HeLa display a significant down-regulation of *SLC25A26* (Fig. 1A). Since DNA methylation is an early and frequent molecular alteration in cervical carcinogenesis with high-risk HPV [2], we performed an *in silico* analysis of the *SLC25A26* promoter gene and identified a CpG island from –370 to –5 bp containing 30 CpG sites. This region was subjected to quantitative bisulfite sequencing analysis using genomic DNA extracted from normal liver tissue, a non-tumoral cell line (HEK293), HeLa cells and CaSki cells. No methylated sites were found in non-tumoral DNA, whereas 13 and 15 methylated sites were found in CaSki and HeLa cells, respectively (Fig. 1B).

To confirm that *SLC25A26* expression was epigenetically regulated, we performed further investigation on CaSki cells that were treated with the methyltransferase inhibitor 5-aza-2′-deoxycytidine (5-Aza), for 48 and 72 h. Subsequent DNA methylation analysis by bisulfite-sequencing revealed a reduction of methylated sites after 48 h incubation time with 5-Aza and the disappearance of methylated sites after 72 h of incubation (Fig. 1C). Consistently, *SLC25A26* mRNA (Fig. 1C) and protein levels (Fig. 1D) gradually increased as the 5-Aza incubation time was raised

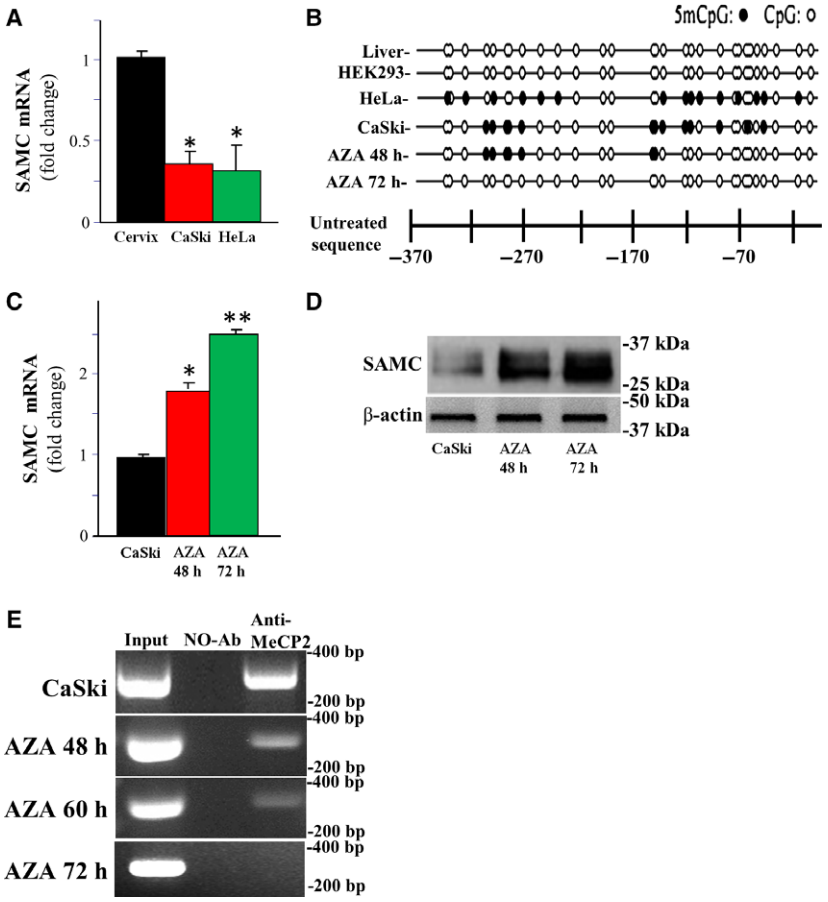

Fig. 1. *SLC25A26* gene is down-regulated in CaSki and HeLa cells through hypermethylation of its promoter. (A) *SLC25A26* gene expression was quantified by real-time PCR in CaSki cells, HeLa cells and cervix tissues (cat. no. AM6992, Thermo Fisher Scientific, Carlsbad, CA, USA). Data are shown as means ± SD of five duplicate independent experiments. $*P < 0.05$ *versus* control (one-way ANOVA). (B) Methylation patterns of the *SLC25A26* gene promoter CpG island in genomic DNA samples from normal liver (cat. no. D1234149, Amsbio, Cambridge, MA, USA), a non-tumoral cell line (HEK293), and HeLa and CaSki cell lines. Where indicated, CaSki cells were treated with 5-Aza for 48 and 72 h. The graphical representation of bisulfite sequencing results was generated by METHTOOLS software (version 1.2) (http://genome.imb-jena.de/ methtools). Bisulfite-generated sequences were compared among them and reported on a base-pair scale. White and black circles indicate unmethylated and methylated cytosine at CpG sites, respectively. (C) *SLC25A26* mRNA levels were quantified by real-time PCR of three independent RNA samples from CaSki cells after treatment with 5-Aza for 48 and 72 h. $*P < 0.05$, $**P < 0.01$, *versus* control (one-way ANOVA). (D) *SLC25A26* protein expression was determined by western blot on lysates from CaSki cells after treatment with 5-Aza for 48 and 72 h. A representative of four blots is shown. (E) Chromatin of CaSki cells was immunoprecipitated by anti-MeCP2 antibody. PCR was performed using forward and reverse primers encompassing the *SLC25A26* gene promoter from −302 to −7 bp. Lane 1, PCR of input DNA dilutions (1/10); lane 2 (No-Ab), PCR of the precipitates without antibody.

(from 48 to 72 h) with respect to untreated CaSki cells. To further confirm the methylation of *SLC25A26* promoter, we tested the ability of methyl CpG binding protein 2 (MeCP2), a global transcriptional repressor, to bind methylated DNA. It is known that this protein binds only to methylated DNA leading to gene silencing, especially in cancer [19]. CaSki cells were treated with 10 μM 5-Aza for 48, 60 and 72 h, and then a chromatin immunoprecipitation (ChIP) experiment was performed on cellular lysates using a specific MeCP2 antibody. A reduction of MeCP2 binding was evident at 48 h and much more so at 60 h. No binding of MeCP2 was observed at 72 h (Fig. 1E).

These results clearly show that promoter hypermethylation is the main cause of *SLC25A26* down-regulation in CaSki cells as compared with untreated cells.

SLC25A26 overexpression affects the mtDNA methylation status in CaSki cells

Based on the observation of reduced *SLC25A26* expression in cervical cancer cells, we employed a re-

expression system to investigate the requirement of low SAMC expression for cancer cell proliferation focusing on mitochondrial functionality. To this aim we transfected CaSki cells with a pcDNA3-SAMC construct containing the *SLC25A26* cDNA (a re-expression system) or with the empty vector (as control). First of all we checked the expression level of SAMC in the transfected CaSki cells (Fig. 2A). Then we evaluated the mitochondrial SAM content by mass spectrometry. As shown in Fig. 2B, the mitochondrial SAM levels were about 50% higher in SAMC-overexpressing CaSki cells than in control cells, suggesting that higher mitochondrial availability of SAM might affect the extent of mtDNA methylation. Next the levels of mtDNA methylation in pcDNA3-SAMC compared with control cells were measured. Notably, the purity of mtDNA was checked with different approaches (see 'Experimental procedures' and Fig. 2C–F). SAMC overexpression led to a 20% increase in mtDNA methylation at 48 h after transfection and reached about 70% increase after 72 h as compared with mtDNA extracted from control CaSki cells (Fig. 2G).

Subsequently the methylation status of the D-loop, the region that controls transcription of mtDNA, was determined. After extraction from control and 48 h/72 h SAMC-overexpressing CaSki cells, mtDNA was bisulfite-modified and used to amplify a portion of D-loop that was subjected to sequencing analysis. After 48 h of transfection all analyzed clones showed identical methylation patterns, with the presence of 11 methylated CpG cytosines in pcDNA3-SAMC transfected CaSki cells, whereas control cells (empty vector) contained only four methylated CpG sites (Fig. 2H). Of note no cytosine outside CpGs was found to be methylated. The percentage of methylated CpG sites was about 40% higher in SAMC-overexpressing compared with control CaSki cells. Surprisingly, after 72 h of transfection the methylation pattern of all analyzed clones was different with only four methylation sites located at CpG sites and all the rest at cytosines outside the CpGs (Fig. 2I). Thus, at 72 h the percentage of methylated cytosines at CpG sites was about 22% higher in SAMC-overexpressing compared with control cells, in which no methylation at both CpG and non-CpG sites was found. The total methylated levels (CpG + non-CpG) in SAMC-overexpressing CaSki cells increased about 100% at 72 h compared with 48 h of transfection. Interestingly, longer exposure to SAMC transfection introduced new mutations in the D-loop of CaSki cells (data not shown) suggesting that a progressive and severe damage of cell functions was underway.

These results clearly indicate that mtDNA and in particular the D-loop control region is hypermethylated due to SAMC overexpression and higher SAM mitochondrial levels.

SLC25A26 overexpression impairs mitochondrial oxidative phosphorylation

To evaluate the consequences of the mtDNA hypermethylation, the expression levels of complex I subunit ND6, a protein under D-loop expression control [20], were determined. As shown in Fig. 3A, the amount of ND6 was reduced after 48 h of transfection with

Fig. 2. Methylation status of mtDNA in SAMC-overexpressing CaSki cells. (A) Expression of SAMC in CaSki cells transfected with empty vector (−) and pcDNA3-SAMC (+). A representative of four blots is shown. (B) SAM was measured in the mitochondria of control and SAMC-overexpressing CaSki cells with mass spectrometry. SAM levels are reported as means ± SD of at least four independent experiments. The significance of the difference between the mitochondrial SAM levels in SAMC-overexpressing compared with control cells is indicated (*$P < 0.05$, one-way ANOVA). (C) Immunoblotting of mitochondrial lysates. (D) Electrophoretic gel of PCR amplifications from mtDNA samples. (E) qPCR graph from mtDNA samples. (F) Electrophoretic gel of mtDNA samples. (G) The total methylation level of mtDNA was obtained by measuring 5-methyl-2′-deoxycytidine (mdC) and 2′-deoxycytidine (dC) in hydrolyzed mtDNA samples isolated from control and SAMC-overexpressing CaSki cells. Data are reported as mdC/(mdC + dC) means ± SD of at least three independent experiments. The significance of the difference between the mdC/(mdC + dC) in SAMC overexpressing compared with control cells is indicated (*$P < 0.05$, one-way ANOVA). (H) Methylation patterns of the mitochondrial D-loop in mtDNA samples from CaSki cells treated with pcDNA3-SAMC for 48 h. The graphical representation was generated as in Fig. 1B. Black circles indicate methylated CpGs sites, white circles the unmethylated CpGs sites, and colored circles refer to methylated cytosines outside CpGs. Lines 1 and 2 indicate methylation of cytosine residues located within CpG nucleotides (CpG methylation); and lines 3 and 4 indicate methylation of cytosine residues located outside of CpG nucleotides (non-CpG methylation). (I) Methylation patterns of the mitochondrial D-loop in mtDNA samples from CaSki cells treated with pcDNA3-SAMC for 72 h. The graphical representation was generated as in Fig. 1B. Black circles indicate methylated CpGs sites, white circles the unmethylated CpGs sites and colored circles methylated cytosines outside CpGs. Lines 5 and 6 indicate methylation of cytosine residues located within CpG nucleotides (CpG methylation); and lines 7 and 8 indicate methylation of cytosine residues located outside CpG nucleotides (non-CpG methylation). New mutations in the D-loop region, which insert or delete cytosines or guanines based on the revised Cambridge reference sequence (rCRS) thus creating or suppressing CpGs, can be ascribed to the adverse conditions for cell survival at 72 h of *SLC25A26* overexpression.

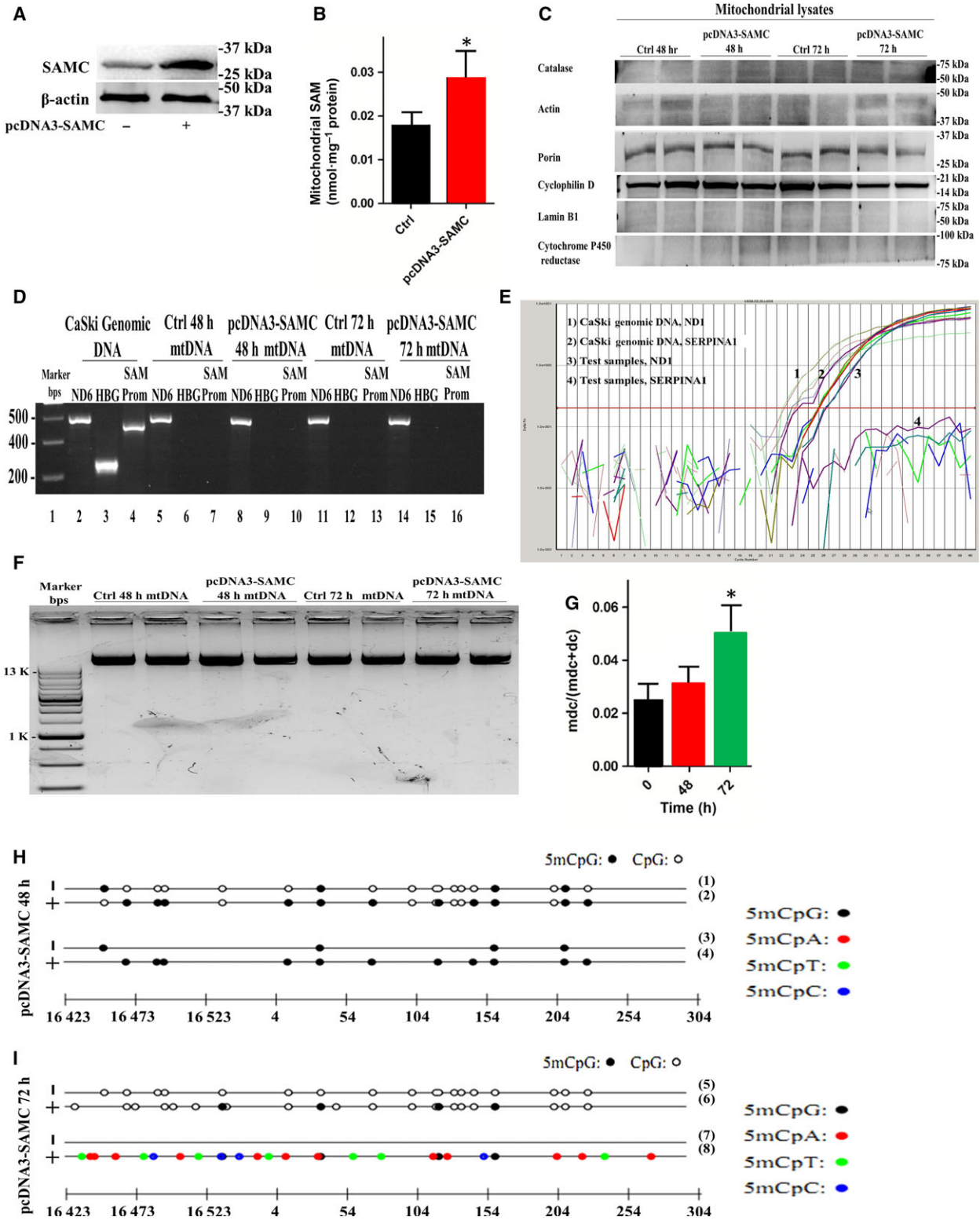
A
SAMC
β-actin
pcDNA3-SAMC
37 kDa
25 kDa
50 kDa
37 kDa
B
Mitochondrial SAM (nmol·mg⁻¹ protein)
Ctrl
pcDNA3-SAMC
C
Mitochondrial lysates
Ctrl 48 hr
pcDNA3-SAMC 48 h
Ctrl 72 h
pcDNA3-SAMC 72 h
Catalase
Actin
Porin
Cyclophilin D
Lamin B1
Cytochrome P450 reductase
D
CaSki Genomic DNA
Ctrl 48 h mtDNA
pcDNA3-SAMC 48 h mtDNA
Ctrl 72 h mtDNA
pcDNA3-SAMC 72 h mtDNA
Marker bps
SAM
ND6 HBG Prom
E
1) CaSki genomic DNA, ND1
2) CaSki genomic DNA, SERPINA1
3) Test samples, ND1
4) Test samples, SERPINA1
F
Marker bps
Ctrl 48 h mtDNA
pcDNA3-SAMC 48 h mtDNA
Ctrl 72 h mtDNA
pcDNA3-SAMC 72 h mtDNA
13 K
1 K
G
mdc/(mdc+dc)
Time (h)
H
5mCpG: ● CpG: ○
pcDNA3-SAMC 48 h
5mCpG:
5mCpA:
5mCpT:
5mCpC:
I
5mCpG: ● CpG: ○
pcDNA3-SAMC 72 h

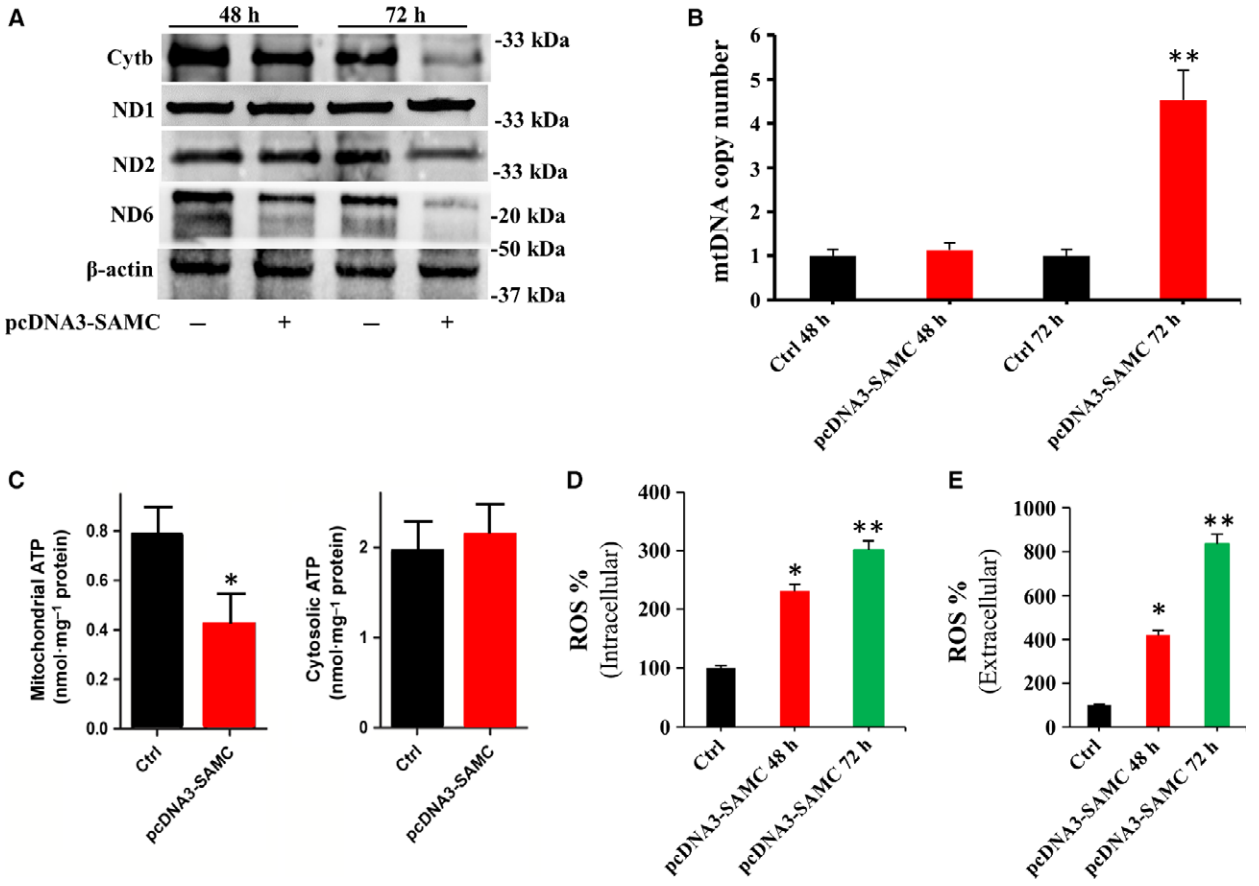

Fig. 3. Effect of SAMC overexpression on ATP production. (A) Cytb, ND1, ND2 and ND6 oxidative phosphorylation chain subunit expression in CaSki cells transfected with pcDNA3-SAMC or with empty vector for 48 and 72 h. β-Actin was used as control. Similar results were obtained in three independent experiments. (B) mtDNA copy number. Real-time PCR was performed using 10 ng of genomic DNA (including mtDNA) from target cells, SYBR Premix Ex Taq™ II (Tli RNaseH Plus) and Human Mitochondrial DNA (mtDNA) Monitoring Primer Set (see TaKaRa protocol). The mtDNA genes ND1 and ND5 were used to represent mtDNA copy number. The values for the controls were set to 1. Data are expressed as means ± SD of three duplicate independent experiments. $^{**}P < 0.01$ (one-way ANOVA). (C) ATP was measured in the mitochondria (left) and post-mitochondrial supernatant (right) of control and SAMC-overexpressing CaSki cells with mass spectrometry analysis. ATP levels are reported as means ± SD of at least four independent experiments. The significance of the difference between the mitochondrial ATP levels in SAMC overexpressing compared with control cells is indicated ($^{*}P < 0.05$, one-way ANOVA). (D,E) Intracellular (D) and extracellular levels (E) of reactive oxygen species (ROS) determined by dichlorodihydrofluorescein and lucigenin after cell transfection with pcDNA3-SAMC for 48 or 72 h. Results are presented as means ± SD from three independent experiments. $^{*}P < 0.05$, $^{**}P < 0.01$ *versus* control (one-way ANOVA).

pcDNA3-SAMC and even more after 72 h as compared with control CaSki cells. This trend was shared by ND2 and cytochrome *b* (Cytb) but not by ND1, the expression of which was unaffected by SAMC overexpression (Fig. 3A). ND6, ND2 and Cytb reduction was not due to a decrease in the mtDNA copy number as a consequence of apoptosis (see below). Indeed, the mtDNA/nuclear DNA ratio was unchanged at 48 h with respect to control cells but increased at 72 h (Fig. 3B), probably due to nuclear DNA degradation [21,22]. The depletion of complex I subunits was confirmed by evaluating the mitochondrial and cytosolic ATP levels by mass spectrometry. Mitochondrial ATP content was reduced by about 50% as compared with control cells indicating that oxidative phosphorylation is impaired in SAMC-overexpressing CaSki cells compared with control cells (Fig. 3C). On the contrary, the cytosolic ATP levels were unchanged following *SLC25A26* overexpression (Fig. 3C) suggesting that glycolytic ATP production is unaffected. In line with these findings, a gradual increase of intracellular and extracellular reactive oxygen species (ROS) levels was observed in SAMC-overexpressing CaSki cells after 48 and 72 h of transfection with respect to control cells (Fig. 3D,E). Therefore, the oxidative phosphorylation impairment caused by

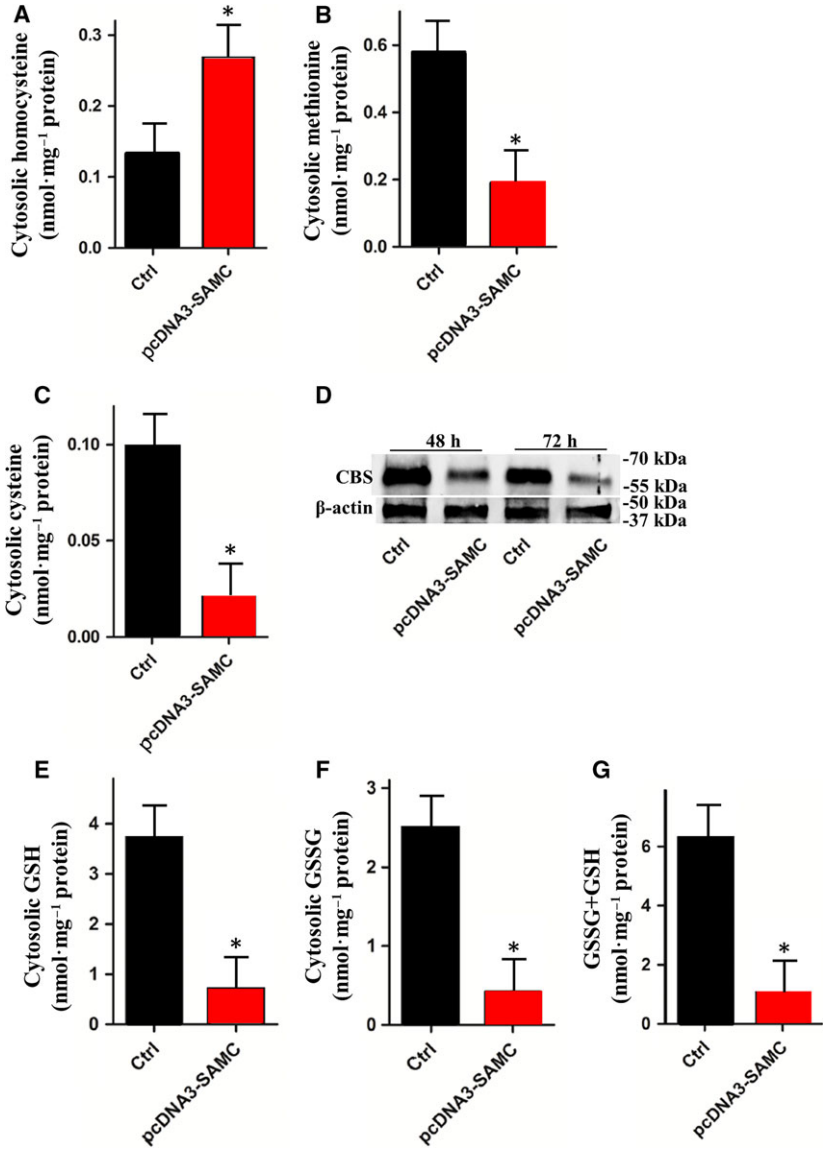

Fig. 4. Effect of SAMC overexpression on the methionine cycle metabolites and glutathione. (A–C) Homocysteine (A), methionine (B) and cysteine (C) were measured in the post-mitochondrial supernatant of control and SAMC-overexpressing CaSki cells with mass spectrometry analysis. Cysteine, homocysteine and methionine levels are reported as means ± SD of at least four independent experiments. The significance of the difference between SAMC-overexpressing compared with control cells is indicated (*$P < 0.05$, one-way ANOVA). (D) CBS expression in control or transfected CaSki cells with pcDNA3-SAMC at 48 and 72 h. β-Actin was used as control. Similar results were obtained in three independent experiments. (E–G) GSH (E), GSSG (F) and the sum of GSSG and GSH (G) were measured in the post-mitochondrial supernatant of control and SAMC-overexpressing CaSki cells. GSSG, GSH and their sum are reported as means ± SD of at least four independent experiments. The significance of the difference between SAMC overexpressing compared with control cells is indicated (*$P < 0.05$, one-way ANOVA).

reduction of ND6, ND2 and Cytb expression is associated with oxidative stress, which may contribute to cell injury.

All together, these results point to a bioenergetic functional failure of the mitochondria in SAMC-overexpressing CaSki cells.

SLC25A26 overexpression reprograms the methionine cycle leading to reduced glutathione level

Since SAM is produced in the cytosol during the conversion of methionine to homocysteine, we questioned

whether increased mitochondrial uptake of SAM (Fig. 2B) can affect the availability of the methyl cycle intermediates. CaSki cells transfected with pcDNA3-SAMC displayed an increase in homocysteine of about 50% (Fig. 4A), a decrease in methionine of about 70% (Fig. 4B) and a decrease in cysteine of about 80% (Fig. 4C). This result correlated with a pronounced reduction expression of CBS, the enzyme responsible for the homocysteine to cystathionine conversion (Fig. 4D). Cytosolic SAM was unchanged (not shown). These data indicate that the methionine cycle is strongly modified by SAMC overexpression. Since the remethylation and transsulfuration pathways are linked by homocysteine, we also evaluated the levels of glutathione, the important non-enzymatic component of the antioxidant defense. As shown in Fig. 4E–G, the levels of both oxidized glutathione (GSSG) and reduced glutathione (GSH) were lower in SAMC-overexpressing CaSki cells compared with control cells, suggesting that the intracellular antioxidant defense of cervical cancer cells is greatly impaired by SAMC overexpression.

SLC25A26 overexpression inhibits cervical cell growth and promotes cell apoptosis

Having established the metabolic effects of SAMC overexpression, we determined its influence on cell growth and proliferation. CaSki cells were transfected with pcDNA3-SAMC or empty vector for 24, 48 and 72 h, and then cell growth was evaluated by the 3-(4,5-dimethylthiazol-2-yl)-2,5-diphenyl-tetrazolium bromide assay. As shown in Fig. 5A, SAMC-overexpressing CaSki cells showed a significantly lower proliferation ability than control cells. Then we assessed at which phase of the cell cycle the growth was arrested by SAMC overexpression. The number of cells measured in each phase showed a more pronounced shift from the G1 to the S phase after 48 h in SAMC-overexpressing cells compared with control cells (Fig. 5B), with a G1 to S phase ratio of 2.98 in control and 1.93 in SAMC-overexpressing cells. After 72 h a dramatic decrease of G1 cells and a drastic increase of S cells occurred (Fig. 5C) resulting in a strong decrease in the G1/S ratio from 2.21 in control to 0.17 in SAMC-overexpressing cells. These results indicate that overexpression of the mitochondrial SAM carrier leads to cellular cycle arrest in the G1–S phase transition. Additionally, after 72 h of pcDNA3-SAMC transfection, the number of viable CaSki cells was reduced from 75.2% in control cells to 48.7% in SAMC-overexpressing cells (Fig. 5D), whereas the percentage of apoptotic cells was increased from 24.8% (control cells) to 51.2% (SAMC-overexpressing CaSki cells) (upper panels of Fig. 5D,E). Consistently, cytosolic release of cytochrome *c*, an indicator of the apoptotic process being executed, significantly increased in pcDNA3-SAMC compared with control CaSki cells (Fig. 5F).

All together these data demonstrate that overexpression of SAMC has deleterious effects on cervical cancer cells growth and proliferation, suggesting that *SLC25A26* could be a novel pro-apoptotic protein.

SLC25A26 overexpression increases the chemosensitivity for cisplatin

Finally, we checked whether *SLC25A26* overexpression effectively sensitizes cells to a well-known chemotherapeutic agent frequently used for cervical cancer, cisplatin (*cis*-diaminodichloro platinum), which acts as an inducer of apoptosis [23]. A 24 h treatment with cisplatin significantly enhanced the apoptotic effect of SAMC overexpression at 72 h, as 93% of cells displayed the apoptotic marker annexin (Fig. 5D,E). Cisplatin treatment alone induced apoptosis in 77% of the control cells, while cisplatin-free SAMC overexpression induced apoptosis in 51.2% of cells (Fig. 5D,E) indicating the additive and combined effect of the chemotherapeutic agent and the SAMC up-regulation on the apoptotic process. Interestingly, the cell cycle G1–S transition was much less evident at both 48 h (56.64%/17.56% = 3.22) and 72 h (48.47%/31.43% = 1.54) in cisplatin-treated compared with untreated pcDNA3-SAMC cells (Fig. 5B,C).

All of these results indicate that SAMC overexpression enhances apoptotic sensitivity to cisplatin-induced cell death.

Discussion

Persistent infection with high-risk types of HPV is known to cause cervical cancer; however, additional genetic and epigenetic alterations are required for progression from a precancerous to invasive state [2]. Promoters of tumor suppressor genes involved in many cellular pathways are methylated in cervical precursors and invasive cancers [2].

In the present study, we demonstrated for the first time that (a) the *SLC25A26* gene is down-regulated in cervical cancer cells CaSki and HeLa by promoter hypermethylation; (b) its overexpression in CaSki cells has a strong impact on cell function by modifying mitochondrial epigenetics and rewiring methyl metabolism. This produces deleterious effects on cell growth and proliferation. Thus, epigenetic suppression of

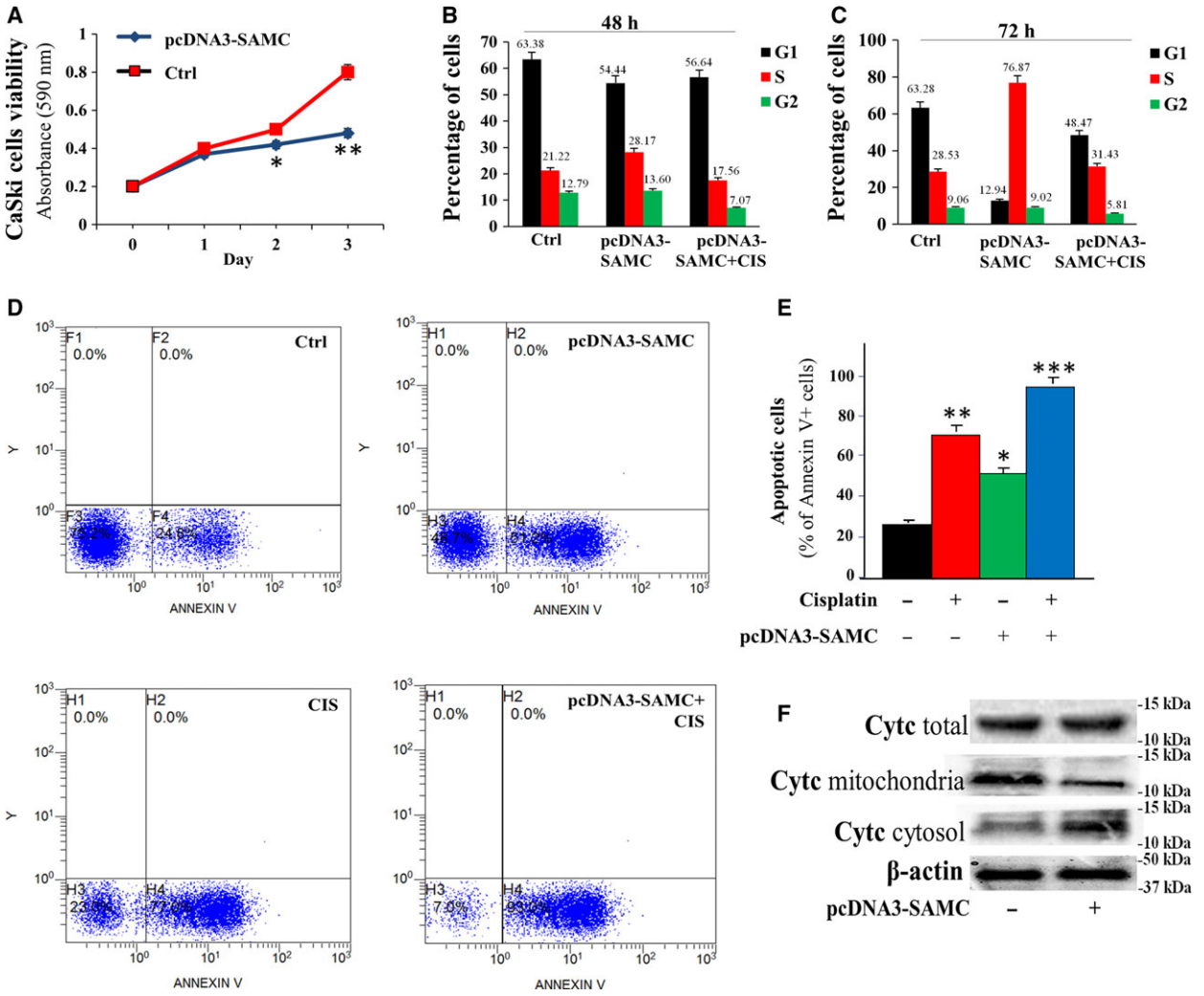

Fig. 5. SAMC overexpression inhibits cell growth and promotes apoptosis. (A) Viability of CaSki cells transfected with pcDNA3-SAMC or with empty vector. Data are expressed as means ± SD of three duplicate independent experiments. $*P < 0.05$, $**P < 0.01$ (one-way ANOVA). (B) The percentage of cells in the G1, S and G2 phase of the cell cycle after 48 h of transfection with pcDNA3-SAMC or pcDNA3-SAMC plus cisplatin. Results are presented as means ± SD from three independent experiments. (C) The percentage of cells in the G1, S and G2 phase of the cell cycle after 72 h of transfection with pcDNA3-SAMC or pcDNA3-SAMC plus cisplatin. Results are presented as means ± SD from three independent experiments. (D) Representative apoptotic cell fraction profiles determined by annexin V staining and analyzed by flow cytometry as described in 'Experimental procedures'. CaSki cells were transfected with pcDNA3-SAMC for 72 h or treated with cisplatin for 24 h or transfected with pcDNA3-SAMC up to 72 h combined with 24 h cisplatin treatment. (E) Percentage of apoptotic cells after transfection and treatment reported in (D). Data are expressed as means ± SD of three duplicate independent experiments. $*P < 0.05$, $**P < 0.01$, $***P < 0.001$ *versus* control (one-way ANOVA). (F) Mitochondrial and cytosolic cytochrome *c* (Cytc) protein content in CaSki cells transfected with pcDNA3-SAMC or empty vector. β-Actin and total cytochrome *c* were used as control. Similar results were obtained in three independent experiments.

SLC25A26 might be part of the epigenetic reprogramming put in action in cervical cancer cells in order to take a selective advantage in survival and growth. Our data highlight also the importance of MeCP2, a global transcriptional repressor binding to methylated DNA and recruiting the SIN3A repressor complex to silence transcription via histone deacetylases [24]. In line with recent reports on the epigenetic role of MeCP2 in different cancers [19], it is likely that MeCP2 is an epigenetic regulator rather than a transcriptional regulator.

In addition, the results presented in this work shed light on the role of methylation of mtDNA, which we not only detected with a very highly sensitive technique but also validated with respect to the D-loop

fragment. mtDNA methylation appears to be strongly dependent on the amount of SAM entering the mitochondria. Intramitochondrial SAM levels over the physiological threshold trigger mtDNA hypermethylation, which leads to oxidative damage and cell injury through reduction or interruption of mitochondrial electron transport and ATP production (Fig. 6). Intramitochondrial SAM is known to be important for ribosome assembly, but the inverse relationship between SAM levels and ND6 expression clearly excludes that the reduction of mitochondrial ATP synthesis, that we detect, is a consequence of impaired ribosome assembly. Furthermore, the observed changes in cells overexpressing SAMC are very unlikely to reflect a lower coenzyme Q synthesis, since higher intramitochondrial SAM levels, which we detect, should result in an increase rather that a decrease of coenzyme Q. Epigenetic modifications of the D-loop produce a specific reduction in the expression of mitochondrial genes, among which are the ND6 and ND2 subunits of the respiratory complex I and the Cytb protein, but not ND1. This differential expression is in line with previous work [25], suggesting that (a) the epigenetic control of ND6, the key limiting peptide for the correct assembly of ND1 and ND2 [26–28], acts as complex I activity modulator; and (b) the mechanism of mitochondrial epigenetic control is gene specific, as pointed out previously [25]. These findings clearly indicate that mitochondrial epigenetics, similarly to the well-established role of nuclear epigenetics, plays an important function in modulating cell life in physiological conditions and in pathological conditions such as cancer. It is noteworthy that, while mitochondrial ATP is significantly reduced by SAMC overexpression, cytosolic ATP remains substantially unchanged. This might indicate that cervical cancer cell bioenergetics is mainly oxidative rather than glycolytic, supporting the idea that not all tumor cell types are energetically dependent on glycolysis [29]. Indeed, bioenergetics of a given type of tumor can widely vary from glycolytic to oxidative depending on the oncogenes activated and the microenvironment [30]. Therefore, the mtDNA methylation profile could help in establishing the cancer cell's bioenergetic profile to improve pharmacological strategies interfering with distinctive steps of cancer energy production pathways [31].

A recent work by Kishita and coworkers [32] describes three patients affected by a rare syndrome caused by recessive mutations of SLC25A26 that impair the transport function of SAMC, which is characterized by mitochondrial defects, including alterations of RNA stability, mitochondrial translation, biosynthesis of coenzyme Q, lipoic acid and ATP synthesis. It is worth noting that this study and ours are hardly comparable given that the two cellular models are very unlike, being from different pathological states. Furthermore, the two models cannot be superimposed since the SAMC-defective patients are characterized by 'loss of function' mutations, whereas SAMC-overexpressing CaSki cells describe a wild-type state with enhanced activity.

The new mutations in the D-loop region are probably related to the adverse conditions for cell survival at 72 h after *SLC25A26* overexpression, among which oxidative stress and apoptosis are known to trigger the appearance of mtDNA mutations [33]. Interestingly, control CaSki cells show apparent CpG methylation at 48 h but not at 72 h. Although the reason for this finding is elusive, one explanation could be found in the nutrient deprivation of the culture medium at 72 h compared with 48 h, in line with a recent research highlighting the role of low nutrient availability in promoting a hypomethylated state [34].

SAMC overexpression in CaSki cells produces deleterious effects, suggesting that *SLCA25A26* could be a novel pro-apoptotic gene in these cancer cells. This unexpected role is based on two main cellular impairments, one dependent on hypermethylation of mtDNA and the other linked to the derangement of the methyl metabolism and decreased availability of GSH (Fig. 6). Increased uptake of SAM into mitochondria forces methionine to be converted to SAM. This causes homocysteine accumulation and GSH depletion (Fig. 6). In fact, the increased mitochondrial SAM uptake is accompanied by a reduction of transsulfuration flux and accumulation of cytosolic homocysteine at the expenses of cysteine and glutathione. High homocysteine is a harmful metabolite, associated with abnormal gene expression and apoptosis [11,35,36], and functionally relevant as an inducer of a shift from the G1 to the S phase in neurons [37], similar to the G1–S transition arrest reported here after SAMC overexpression in CaSki cells. On the other hand, reduction of glutathione, the major non-enzymatic component of the intracellular antioxidant defense, is destined to increase oxidative damage, which is known to lead to a progressive cell transit into S phase, DNA damage and blockade of the cell cycle resulting in apoptosis [38]. Indeed, we found an increase of ROS production following SAMC overexpression, which could be a consequence of the redox dyshomeostasis and the failure of the antioxidant endogenous defense (Fig. 6). It is known that ROS can be pro-tumorigenic, but also increase the susceptibility of cancer cells to death. Therefore, the amount of ROS produced by cancer

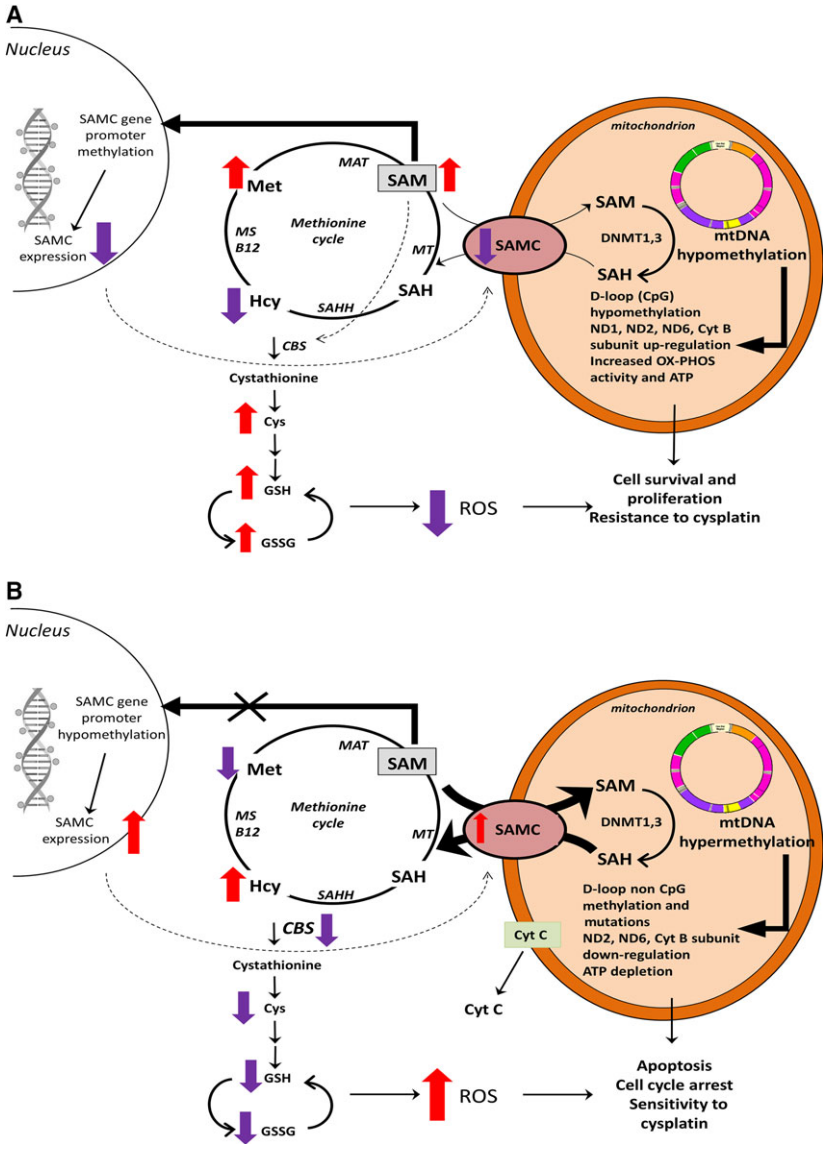

Fig. 6. Schematic pathways related to *SLC25A26* expression. (A) *SLC25A26* gene down-regulation in CaSki cells. SAMC down-regulation by epigenetic suppression of *SLC25A26* gene promoter induces cancer cell survival by channeling the methyl cycle toward GSH synthesis. Lower mitochondrial SAM availability maintains mtDNA in a lower methylation state, promoting oxidative phosphorylation and ATP synthesis. (B) *SLC25A26* gene overexpression in CaSki cells induces a withdrawal of SAM into mitochondria, leading to mtDNA hypermethylation, repression of oxidative phosphorylation and decreased mitochondrial ATP. Mitochondrial SAM uptake forces homocysteine to channel into the methyl cycle at the expense of GSH synthesis by CBS down-regulation. Increased homocysteine and reduced GSH weaken cells against ROS production thus leading to cell cycle arrest and apoptosis. Downward and upward thick arrows indicate reduction and increase, respectively. Thin arrows indicate the metabolic pathway. Main biological effects of hypo/hypermethylation are highlighted. Hcy, homocysteine; MAT, methionine adenosyltransferase; MS, methionine synthase; MT, methyltransferase; SAH, *S*-adenosylhomocysteine; SAHH, SAH hydrolase.

cells must be maintained below the threshold that induces cell death [39]. Strong evidence links GSH levels, cancer growth and resistance. A direct correlation between GSH levels, proliferation and metastatic activity has been highlighted [21,40,41]. Up-regulation of GSH synthesis and GSH synthesizing enzymes has been noted in many cancer tissues [42–44] to the point that a higher GSH synthesizing potential in cancer cells is considered an adverse prognostic indicator [44]. GSH synthesis has also been indicated as a mechanism

mediating cancer cells' resistance to cisplatin. Metabolic data point to a metabolic reprogramming of cancer cell metabolism toward GSH synthesis as a mechanism to increase cell survival and escape toxicity of chemotherapeutic agents [45]. Epigenetic down-regulation of SAMC gene could represent one of the events put in action by cancer cells to increase GSH synthesis (Fig. 6). This hypothesis is supported by the levels of CBS expression, which progressively decrease as a consequence of SAMC up-regulation (Fig. 6). In fact, CBS down-regulation might represent a compensatory mechanism that represses homocysteine to cystathionine conversion in an attempt to favor homocysteine channeling into SAM synthesis, required to support mitochondrial uptake, at the expenses of cysteine, and thus of GSH production. Furthermore, CBS is also sensitive to ROS attack [46] pointing to oxidative stress induced by SAMC overexpression as an additional mechanism exacerbating reduction of CBS enzymatic activity, leading to further homocysteine accumulation.

Another aspect of SAMC overexpression in CaSki cells concerns the sensitivity to cisplatin, a drug often used to treat advanced cervical cancer. The increased chemosensitivity to cisplatin could be related to the decreased level of glutathione (see above). Both pcDNA3-SAMC transfection and cisplatin treatment exert a combined effect on the apoptotic process [47]. The mechanisms by which SAMC and cisplatin are mutually reinforcing are not known. Since cisplatin is able to shift cancer cell metabolism from glycolysis to oxidative phosphorylation [48,49], it may be that the bioenergetic perturbation of oxidative phosphorylation, mediated by SAMC overexpression, could be the basis of the reinforcing apoptotic effect.

The results of our study demonstrate for the first time that increased SAM influx into mitochondria, due to SAMC overexpression, affects mtDNA methylation and mitochondrial function leading to impairment of oxidative phosphorylation, increased oxidative stress, decrease in GSH defense and apoptosis. Therefore, CaSki cervical cancer cells have an advantage in down-regulation of *SLC25A26*, which occurs through epigenetic hypermethylation of its promoter. These findings highlight that mitochondrial epigenetics might play an important role in cancer growth and progression. Thus, epigenetic modifications of mtDNA cannot be relegated to a secondary mechanism of regulation of transcription and protein synthesis in the organelles, representing a fundamental process able to influence the whole cell life in normal and pathological conditions including cancer.

Experimental procedures

Culture of CaSki cells and fractionation

CaSki cells (ATCC CRL-1550™, ATCC, Manassas, VA, USA) were grown in RPMI-1640 medium (ATCC 30-2001™, ATCC) with 10% fetal bovine serum (ATCC 30-2020™, ATCC), 2 mM L-glutamine and 1% penicillin/streptomycin (cat. no. P4333, Sigma-Aldrich, St Louis, MO, USA) at 37 °C in a humidified atmosphere with 5% CO_2. For cell fractionation 2×10^7 cells of each sample were lysed within a Dounce tissue grinder (cat no. D8938, Sigma-Aldrich) in the presence of the lysis buffers provided by the Mitochondria Isolation Kit for Cultured Cells (cat. no. 89874, Thermo Fisher Scientific, Waltham, MA, USA); and the mitochondria were collected by differential centrifugation [25,50]. Protein content was determined by using the Bradford protein assay (cat. no. 23236, Pierce/Thermo Fisher Scientific).

Treatments

Where indicated, CaSki cells were incubated with 20 μM cisplatin (a gift from F. Intini, University of Bari, Bari, Italy) for 24 h [51] or with 10 μM 5-Aza (cat. no. A2385, Sigma-Aldrich) up to 72 h [52]. The medium containing the drug or vehicle was replaced every 24 h during a 72-h period.

Construction of expression vector harboring SAMC complete coding sequence

One microgram of Human Testes Total RNA (cat. no. AM7972, Thermo Fisher Scientific) was reverse transcripted with GeneAmp RNA PCR core kit (cat. no. N8080143, Thermo Fisher Scientific) as described previously [53]. The full-length coding region of the human *SLC25A26* (GenBank accession number NM_173471.3) was amplified from testes cDNA using the iProof High Fidelity DNA Polymerase (cat. no. 1725302, Bio-Rad, Hercules, CA, USA) and the primers listed in Table 1 in a final volume of 50 μL [54]. The PCR amplification product was purified using the High Pure PCR Product Purification Kit (cat. no. 11732668001, Roche Life Science, Indianapolis, IN, USA) and ligated with pcDNA3.1(+) vector (V790-20, Thermo Fisher Scientific) in the sense orientation. The fidelity of the human *SLC25A26* insert in the pcDNA3.1(+) plasmid was verified by DNA sequencing using Big Dye Terminator Kit (cat. no. 4337455, Thermo Fisher Scientific).

Transient transfection

CaSki cells were transfected with the pcDNA3.1(+) vector containing the target *SLC25A26* cDNA by FuGENE® HD

Table 1. Nucleotide sequences of primers used for the experiments.

Gene	Forward primer (5′ to 3′)	Reverse primer (5′ to 3′)
*SLC25A26*_cDNA	CAGGAATTCATGGACCGGCCGGGGTTCGTGG	CGACTCGAGTCAAGGACTCTTTCTGCCAACT
Human beta-globin	CAACTTCATCCACGTTCACC	GAAGAGCCAAGGACAGGTAC
SLC25A26 gene promoter	AGATAAACCAAAATGAAATATCC	TCAGACCTCGTCAAGGCTACAAT
ND6	TCCTCCTAGACCTAACCTGA	GGATATACTACAGCGATGG
−302 to −7 bp region of the *SLC25A26* gene promoter	ACGGATCTTTTGCTCGCGAAAGTT	TCAGACCTCGTCAAGGCTACAAT
16423–256 bp region of the D-loop	GATAGGGGTTTTTTGATTATTATTTTT	ACAAACATTCAATTATTATTATTATATCCT
−370 to +1 bp region of the *SLC25A26* gene promoter	TTTTTTTGGGTTTATAGTTTAGAATTA	ACAATACAAACATAACCTTAACACCT

Transfection Reagent (cat. no. E2311, Promega, Madison, WI, USA) as previously described [55] with some modifications. In brief, CaSki cells were plated 18–24 h prior to transfection, so that the monolayer cell density reached the optimal of ~ 90% confluency at the time of transfection, in a T-150 flask (cat. no. CLS430825, Sigma- Aldrich) and grown in 47 mL of RPMI medium. The mixture of plasmid (52 μg) and transfection reagent (157 μL) in Opti-MEM medium (cat. no. 31985062, Thermo Fisher Scientific) was added to the culture and the cells were incubated for 48/72 h and then used in the experiments. The transfection efficiency was analyzed by immunoblotting with anti-SAMC antibody (1 : 500, cat. no. ab 182103, Abcam, Cambridge, MA, USA). Where indicated, transfected cells were also treated with cisplatin for 24 h at the concentration of 20 μM [51].

Cell viability

Viability of CaSki cells transfected with pcDNA3-SAMC up to 72 h was evaluated as described previously [56].

Flow cytometry analysis of the cell cycle

CaSki cells transfected with pcDNA3-SAMC and, where indicated, treated with cisplatin were harvested and washed twice with PBS. After fixing the cells in cold 70% ethanol at 4 °C overnight, the cells were washed, resuspended in cold PBS and incubated with 10 $mg{\cdot}mL^{-1}$ RNase (cat. no. EN0531, Thermo Fisher Scientific) and 1 $mg{\cdot}mL^{-1}$ propidium iodide (PI) (cat. no. P3566, Thermo Fisher Scientific) at 37 °C for 30 min in the dark. The samples were analyzed by flow cytometry (BD Biosciences, San Diego, CA, USA), and the percentage of cells in the G0/G1, S and G2/M phases was determined using Cell Quest acquisition software (BD Biosciences) as described [57].

Annexin V-FITC flow cytometric analysis for apoptotic cell death

CaSki cells transfected with pcDNA3-SAMC and, where indicated, treated with cisplatin were harvested, washed twice with ice-cold PBS and resuspended at a density of 1×10^6 $cells{\cdot}mL^{-1}$ in 100 μL of binding buffer containing 5 μL of annexin V/FITC (cat. no. A13199, Thermo Fisher Scientific). After incubation at room temperature for 15 min in the dark, 400 μL of binding buffer was added to each sample. Apoptosis was analyzed by flow cytometry (BD Biosciences) for at least 10 000 events as described [57].

Bisulfite treatment

Bisulfite conversion of 300 ng of genomic DNA or purified mtDNA was performed by using the EZ DNA Methylation-Direct Kit (cat. no. D5021, Zymo Research, Irvine, CA, USA) according to the manufacturer's protocol. To ensure that cytosine conversion was complete, alternative bisulfite modifications were performed by using the EZ DNA Methylation-Gold Kit (cat. no. D5006, Zymo Research) and the Cells-to-CpG™ Bisulfite Conversion Kit (cat. no. 4445554, Thermo Fisher Scientific) according to the manufacturer's protocol. The effectiveness of the entire experimental procedure was also evaluated by analyzing CpGenome™ Universal Unmethylated DNA (cat. no. S7821, Sigma-Aldrich). For each procedure of bisulfite treatment, unconverted primers randomly covering the entire mtDNA molecule, including those used for the D-loop analysis, were used in polymerase chain reactions (PCR), as negative controls [18].

ROS detection

For intracellular ROS analysis, CaSki cells transfected with pcDNA3-SAMC for 48 and 72 h were incubated with 10 μM 2′,7′-dichlorodihydrofluorescein diacetate (cat. no. D399, Thermo Fisher Scientific) for 30 min [58]. For extracellular ROS analysis, CaSki cells transfected as described above in RPMI-modified medium without phenol red (cat. no. R8755, Sigma-Aldrich) were treated with 0.2 mM lucigenin (Alexis, Loerrach, Germany) [59]. The fluorescence and the chemiluminescence resulting from ROS were analyzed using a microplate reader (Victor X3; Perkin Elmer, Waltham, MA, USA).

Quantification of cytosolic and mitochondrial metabolites by mass spectrometry

Quantification of cytosolic and mitochondrial metabolites was performed as reported previously [15,60–62] with some modifications. Flash mitochondrial isolation was performed as indicated [15,61]. Mitochondria (0.5 mg of proteins), used for SAM and ATP quantification, and 1 mL of post-mitochondrial supernatant were extracted with chloroform. A Quattro Premier mass spectrometer interfaced with an Acquity UPLC system (Waters, Milford, MA, USA) was used for liquid chromatography–tandem mass spectrometry analysis. The multiple reaction monitoring transitions in the positive ion mode were m/z 399.1 > 250.1 for SAM, m/z 121.9 > 76.1 for cysteine, m/z 136.1 > 90.1 for homocysteine, m/z 150.0 > 56.1 for methionine, m/z 308.1 > 179.0 for GSH, and m/z 613.2 > 484.2 for GSSG. For ATP quantification, the m/z measured in the single ion recording mode was 506.0 m/z in the negation ion mode. Calibration curves were established using standards, processed under the same conditions as the samples, at five concentrations [63,64]. The best fit was determined using regression analysis of the peak analyte area.

Real-time PCR

Total RNA was extracted from 1×10^6 CaSki and HeLa (ATCC CCL2™, ATCC) cells by GenElute Mammalian Total RNA Miniprep Kit (cat. no. RTN70**,** Sigma-Aldrich) and transcribed by reverse transcriptase. Cervix cDNAs were prepared by reverse transcription of total RNA from Human Cervix (cat. no. AM6992, Thermo Fisher Scientific). Then real-time PCR was carried out as reported [65]. Assay-on-demand for human SAMC (cat. no. Hs00384779_m1) and human β-actin (cat. no. Hs99999903_m1) were purchased from Thermo Fisher Scientific. The transcript levels were normalized against the expression levels of β-actin.

Isolation of nuclear and purified mitochondrial DNA

Genomic DNA was isolated with the GenElute Mammalian Genomic DNA Miniprep Kit (cat. no. G1N350, Sigma-Aldrich). Purified mitochondria (see 'Culture of CaSki cells and fractionation') were pre-treated with DNase I (cat. no. AM2222, Thermo Fisher Scientific) in 3 μL incubation buffer (10×, 400 mM Tris/HCl, 100 mM NaCl, 60 mM $MgCl_2$, 10 mM $CaCl_2$; pH 7.9) for 3 h at 37 °C to avoid nuclear DNA contamination. Then mtDNA was isolated with mtDNA Isolation Kit (K280-50, BioVision, Milpitas, CA, USA). mtDNA concentration and purity were determined by electrophoresis on a 0.7% agarose gel and by measuring A_{260} and A_{280} and calculating the A_{260}/A_{280} ratio [15,66]. To further rule out contamination with nuclear DNA, PCRs were performed to detect two specific nuclear DNA regions (human beta-globin and *SLC25A26* gene promoter) and one from the mitochondrial genome (ND6) [67] using the primers listed in Table 1. Furthermore, a real-time PCR was performed using SYBR® Premix Ex Taq™ II Tli RNaseH Plus (cat. no. RR82LR, Clontech, Mountain View, CA, USA) and ND1, SERPINA1 primers from Human Mitochondrial DNA (mtDNA) Monitoring Primer Set® (cat. no. 7246, Clontech). CaSki genomic DNA (nuclear DNA plus mtDNA) was used as positive control.

mtDNA copy number

To quantify mtDNA copy number, real-time PCR was performed using 10 ng of genomic DNA (including mtDNA) from target cells, SYBR® Premix Ex Taq™ II Tli RNaseH Plus (cat. no. RR82LR, Clontech) and Human Mitochondrial DNA (mtDNA) Monitoring Primer Set® (cat. no. 7246, Clontech). The relative mtDNA copy number was defined as the total amount of mtDNA divided by the total amount of nuclear DNA.

Quantification of mtDNA methylation

Mitochondrial DNA (about 2 μg) was digested by nuclease S1 (cat. no. EN0321, Thermo Fisher Scientific), phosphodiesterase I (cat. no. P3243, Sigma-Aldrich) and alkaline phosphatase (APMB-RO, Roche Life Science) [15,68]. For mass spectrometry analysis of 5-methyl-2′-deoxycytidine (mdC) and 2′-deoxycytidine (dC), using 2′-deoxyguanosine (dG) as internal standard [15], the following multiple reaction monitoring transitions were identified as follows: m/z 242.10 > 126.10 for mdC, m/z 228.10 > 112.10 for dC and m/z 268.1 > 152.3 for dG [15]. Calibration curves were established using standards, processed under the same conditions as the samples, at five concentrations [63,64,69]. The best fit was determined using regression analysis of the peak analyte area.

Chromatin immunoprecipitation

ChIP experiments were performed as previously reported [58]. Briefly, 2×10^7 CaSki cells exposed up to 72 h to 10 μM 5-Aza were fixed by 1% formaldehyde at 37 °C for 10 min; afterwards, the cells were lysed and sheared by sonication in a 1% SDS lysis buffer to generate cellular chromatin fragments of 400–500 bp. The chromatin was immunoprecipitated for 14–16 h at 4 °C using a specific antibody to MeCP2 (cat. no. SAB4800012, Sigma-Aldrich). After reverse cross-linking, chromatin immunoprecipitates were purified and 2 μL of each sample was analyzed by PCR using the primers listed in Table 1, suitable to amplify the −302 to −7 bp region of the *SLC25A26* gene promoter.

Bisulfite sequencing

For DNA methylation analysis, bisulfite-modified DNA was amplified with specific primers using TaKaRa Epi-Taq™ HS (cat. no. R110A, Clontech). Mitochondrial DNA was amplified at the D-loop using the primers listed in Table 1. The −370 to +1 bp region of the *SLC25A26* gene promoter was amplified using the primers listed in Table 1. PCR was run under the following conditions: preincubation at 98 °C for 10 s, run for 40 cycles at 98 °C for 10 s, 55 °C for 30 s, and 72 °C for 30 s, extension at 72 °C for 5 min. The PCR products, purified by High Pure PCR Product Purification Kit (cat. no. 11732668001, Roche Life Science), were cloned into pCR4-TOPO® Vector (cat. no. K457502, Thermo Fisher Scientific) according to the manufacturer's protocol. Fifteen positive clones per sample were analyzed. Plasmids were purified using PureLink Quick Plasmid Miniprep Kit (cat. no. K457502, Thermo Fisher Scientific) and analyzed by automated sequencing in an ABI PRISM 310 (Thermo Fisher Scientific) with the Big Dye Terminator Cycle Sequencing Ready Reaction Kit (cat. no. 4337455, Thermo Fisher Scientific).

Primer design for PCR reactions

For DNA methylation analysis primers were designed using METHPRIMER Software (http://www.urogene.org/methprimer/index1.html). Some precautions were taken for primer design: (a) cytosines within CpG sites were avoided; (b) where possible, DNA regions characterized by low polymorphism content were preferred; (c) a short size of the amplicons was defined (range: 350–550 bp); (d) generally 26–32 bases are required; (e) annealing temperatures of 55–60 °C were preferred.

Other methods

For western blotting analysis, proteins were electroblotted onto nitrocellulose membranes (cat. no. 1620112, Bio-Rad), and subsequently treated with the following antibodies: rabbit polyclonal anti-cytochrome P450 reductase (cat. no. ab13513, Abcam) at 1 : 1000; mouse monoclonal anti-actin (cat. no. MAB1501, Sigma-Aldrich) at 1 : 1000; mouse monoclonal anti-porin (cat. no. ab14734, Abcam) at 1 : 3000; rabbit polyclonal anti-lamin (cat. no. ab26300, Abcam) at 1 : 500; mouse monoclonal anti-catalase (cat. no. C0979, Sigma-Aldrich) at 1 : 2000; rabbit anti-cyclophilinD (cat. no. GTX79245, Genetex, Irvine, CA, USA) at 1 : 3000; anti-SAMC (cat. no. ab 182103, Abcam) at 1 : 500; rabbit anti-ND6 (cat. no. sc-20510-R, Santa Cruz Biotechnology, Dallas, TX, USA) at 1 : 500; rabbit polyclonal anti-ND2 (cat. no. PA5-37185, Thermo Fisher Scientific) at 1 : 500; rabbit polyclonal anti-ND1 (cat. no. PA5-36493, Thermo Fisher Scientific) at 1 : 500; rabbit polyclonal anti-Cytb (PA5-26626, Thermo Fisher Scientific) at 1 : 500; mouse anti-cytochrome *c* (cat. no. sc-13560, Santa Cruz Biotechnology) and mouse monoclonal anti-β-actin (cat. no. sc-47778, Santa Cruz Biotechnology). The immunoreactions were detected by the SuperSignal™ West Pico Chemiluminescent Substrate (cat. no. 34080, Thermo Fisher Scientific).

Statistical analysis

Statistical significance of differences was determined using one-way ANOVA. Data are expressed as means ± standard deviation and differences were considered as significant ($*P < 0.05$); very significant ($**P < 0.01$) and highly significant ($***P < 0.001$).

Acknowledgements

The authors thank Dr F. Intini, University of Bari, Bari, Italy for supplying cisplatin. This research received funding from the Italian Ministry of Education, Universities and Research (MIUR) and the University of Bari 'Aldo Moro'.

Author contributions

VI, AC, FP and AM designed the research. AM is responsible for the execution and design of most experiments. VI, AC and AM analyzed the data. EMP, AC, VI, MM and AS contributed to the execution of some experiments. VI, AC, AM and FP wrote the paper.

References

1 Kaelin WG & McKnight SL (2013) Influence of metabolism on epigenetics and disease. *Cell* **153**, 56–69.
2 Yang H-J (2013) Aberrant DNA methylation in cervical carcinogenesis. *Chin J Cancer* **32**, 42–48.
3 Jeong DH, Youm MY, Kim YN, Lee KB, Sung MS, Yoon HK & Kim KT (2006) Promoter methylation of p16, DAPK, CDH1, and TIMP-3 genes in cervical cancer: correlation with clinicopathologic characteristics. *Int J Gynecol Cancer* **16**, 1234–1240.
4 Cavalcante JR, Sampaio JPA, Maia Filho JTA, Vieira RB, Eleutério J, Lima RCP, Ribeiro RA & Almeida PRC (2014) Progressive loss of E-cadherin immunoexpression during cervical carcinogenesis. *Acta Cir Bras* **29**, 667–674.
5 Chen CL, Liu SS, Ip SM, Wong LC, Ng TY & Ngan HYS (2003) E-cadherin expression is silenced by DNA methylation in cervical cancer cell lines and tumours. *Eur J Cancer* **39**, 517–523.
6 Overmeer RM, Louwers JA, Meijer CJLM, van Kemenade FJ, Hesselink AT, Daalmeijer NF, Wilting

SM, Heideman DAM, Verheijen RHM, Zaal A *et al.* (2011) Combined CADM1 and MAL promoter methylation analysis to detect (pre-)malignant cervical lesions in high-risk HPV-positive women. *Int J Cancer* **129**, 2218–2225.
7 Overmeer RM, Henken FE, Snijders PJF, Claassen-Kramer D, Berkhof J, Helmerhorst TJM, Heideman DAM, Wilting SM, Murakami Y, Ito A *et al.* (2008) Association between dense CADM1 promoter methylation and reduced protein expression in high-grade CIN and cervical SCC. *J Pathol* **215**, 388–397.
8 Palmieri F (2013) The mitochondrial transporter family SLC25: identification, properties and physiopathology. *Mol Asp Med* **34**, 465–484.
9 Palmieri F (2014) Mitochondrial transporters of the SLC25 family and associated diseases: a review. *J Inherit Metab Dis* **37**, 565–575.
10 Agrimi G, Di Noia MA, Marobbio CM, Fiermonte G, Lasorsa FM & Palmieri F (2004) Identification of the human mitochondrial S-adenosylmethionine transporter: bacterial expression, reconstitution, functional characterization and tissue distribution. *Biochem J* **379**, 183–190.
11 Iacobazzi V, Infantino V, Castegna A & Andria G (2014) Hyperhomocysteinemia: Related genetic diseases and congenital defects, abnormal DNA methylation and newborn screening issues. *Mol Genet Metab* **113**, 27–33.
12 Wallace DC & Fan W (2010) Energetics, epigenetics, mitochondrial genetics. *Mitochondrion* **10**, 12–31.
13 Prudova A, Bauman Z, Braun A, Vitvitsky V, Lu SC & Banerjee R (2006) S-adenosylmethionine stabilizes cystathionine beta-synthase and modulates redox capacity. *Proc Natl Acad Sci USA* **103**, 6489–6494.
14 Mishra M & Kowluru RA (2015) Epigenetic modification of mitochondrial DNA in the development of diabetic retinopathy. *Invest Ophthalmol Vis Sci* **56**, 5133–5142.
15 Infantino V, Castegna A, Iacobazzi F, Spera I, Scala I, Andria G & Iacobazzi V (2011) Impairment of methyl cycle affects mitochondrial methyl availability and glutathione level in Down's syndrome. *Mol Genet Metab* **102**, 378–382.
16 Iacobazzi V, Castegna A, Infantino V & Andria G (2013) Mitochondrial DNA methylation as a next-generation biomarker and diagnostic tool. *Mol Genet Metab* **110**, 25–34.
17 Castegna A, Iacobazzi V & Infantino V (2015) The mitochondrial side of epigenetics. *Physiol Genomics* **47**, 299–307.
18 Bellizzi D, D'aquila P, Scafone T, Giordano M, Riso V, Riccio A & Passarino G (2013) The control region of mitochondrial DNA shows an unusual CpG and non-CpG methylation pattern. *DNA Res.* **20**, 537–547.
19 Parry L & Clarke AR (2011) The roles of the methyl-CpG binding proteins in cancer. *Genes Cancer* **2**, 618–630.
20 Pirola CJ, Gianotti TF, Burgueño AL, Rey-Funes M, Loidl CF, Mallardi P, Martino JS, Castaño GO & Sookoian S (2013) Epigenetic modification of liver mitochondrial DNA is associated with histological severity of nonalcoholic fatty liver disease. *Gut* **62**, 1356–1363.
21 Marengo B, De Ciusis C, Ricciarelli R, Romano P, Passalacqua M, Marinari UM, Pronzato MA & Domenicotti C (2010) DNA oxidative damage of neoplastic rat liver lesions. *Oncol Rep* **23**, 1241–1246.
22 Murgia M, Pizzo P, Sandona D, Zanovello P, Rizzuto R & Di Virgilio F (1992) Mitochondrial DNA is not fragmented during apoptosis. *J Biol Chem* **267**, 10939–10941.
23 Wang D & Lippard SJ (2005) Cellular processing of platinum anticancer drugs. *Nat Rev Drug Discov* **4**, 307–320.
24 Nan X, Ng HH, Johnson CA, Laherty CD, Turner BM, Eisenman RN & Bird A (1998) Transcriptional repression by the methyl-CpG-binding protein MeCP2 involves a histone deacetylase complex. *Nature* **393**, 386–389.
25 Shock LS, Thakkar PV, Peterson EJ, Moran RG & Taylor SM (2011) DNA methyltransferase 1, cytosine methylation, and cytosine hydroxymethylation in mammalian mitochondria. *Proc Natl Acad Sci USA* **108**, 3630–3635.
26 Vartak R, Deng J, Fang H & Bai Y (2015) Redefining the roles of mitochondrial DNA-encoded subunits in respiratory Complex I assembly. *Biochim Biophys Acta* **1852**, 1531–1539.
27 Bai Y & Attardi G (1998) The mtDNA-encoded ND6 subunit of mitochondrial NADH dehydrogenase is essential for the assembly of the membrane arm and the respiratory function of the enzyme. *EMBO J* **17**, 4848–4858.
28 Chomyn A (2001) Mitochondrial genetic control of assembly and function of complex I in mammalian cells. *J Bioenerg Biomembr* **33**, 251–257.
29 Moreno-Sánchez R, Rodríguez-Enríquez S, Marín-Hernández A & Saavedra E (2007) Energy metabolism in tumor cells. *FEBS J* **274**, 1393–1418.
30 Jose C, Bellance N & Rossignol R (2011) Choosing between glycolysis and oxidative phosphorylation: a tumor's dilemma? *Biochim Biophys Acta* **1807**, 552–561.
31 Gogvadze V, Zhivotovsky B & Orrenius S (2010) The Warburg effect and mitochondrial stability in cancer cells. *Mol Aspects Med* **31**, 60–74.
32 Kishita Y, Pajak A, Bolar NA, Marobbio CMT, Maffezzini C, Miniero DV, Monné M, Kohda M, Stranneheim H, Murayama K *et al.* (2015) Intra-mitochondrial methylation deficiency due to mutations in SLC25A26. *Am J Hum Genet* **97**, 761–768.

33 Mambo E, Gao X, Cohen Y, Guo Z, Talalay P & Sidransky D (2003) Electrophile and oxidant damage of mitochondrial DNA leading to rapid evolution of homoplasmic mutations. *Proc Natl Acad Sci USA* **100**, 1838–1843.
34 Zheng LD, Linarelli LE, Liu L, Wall SS, Greenawald MH, Seidel RW, Estabrooks PA, Almeida FA & Cheng Z (2015) Insulin resistance is associated with epigenetic and genetic regulation of mitochondrial DNA in obese humans. *Clin Epigenetics* **7**, 60.
35 Linnebank M, Lutz H, Jarre E, Vielhaber S, Noelker C, Struys E, Jakobs C, Klockgether T, Evert BO, Kunz WS *et al.* (2006) Binding of copper is a mechanism of homocysteine toxicity leading to COX deficiency and apoptosis in primary neurons, PC12 and SHSY-5Y cells. *Neurobiol Dis* **23**, 725–730.
36 Outinen PA, Sood SK, Pfeifer SI, Pamidi S, Podor TJ, Li J, Weitz JI & Austin RC (1999) Homocysteine-induced endoplasmic reticulum stress and growth arrest leads to specific changes in gene expression in human vascular endothelial cells. *Blood* **94**, 959–967.
37 Ye W & Blain SW (2010) S phase entry causes homocysteine-induced death while ataxia telangiectasia and Rad3 related protein functions anti-apoptotically to protect neurons. *Brain* **133**, 2295–2312.
38 Circu ML & Aw TY (2012) Glutathione and modulation of cell apoptosis. *Biochim Biophys Acta* **1823**, 1767–1777.
39 Huang P, Feng L, Oldham EA, Keating MJ & Plunkett W (2000) Superoxide dismutase as a target for the selective killing of cancer cells. *Nature* **407**, 390–395.
40 Carretero J, Obrador E, Anasagasti MJ, Martin JJ, Vidal-Vanaclocha F & Estrela JM (1999) Growth-associated changes in glutathione content correlate with liver metastatic activity of B16 melanoma cells. *Clin Exp Metastasis* **17**, 567–574.
41 Carretero J, Obrador E, Esteve JM, Ortega A, Pellicer JA., Sempere FV & Estrela JM (2001) Tumoricidal activity of endothelial cells: inhibition of endothelial nitric oxide production abrogates tumor cytotoxicity induced by hepatic sinusoidal endothelium in response to B16 melanoma adhesion in vitro. *J Biol Chem* **276**, 25775–25782.
42 Täger M, Ittenson A, Franke A, Frey A, Gassen HG & Ansorge S (1995) gamma-Glutamyl transpeptidase-cellular expression in populations of normal human mononuclear cells and patients suffering from leukemias. *Ann Hematol* **70**, 237–242.
43 Obrador E, Carretero J, Ortega A, Medina I, Rodilla V, Pellicer JA & Estrela JM (2002) Gamma-glutamyl transpeptidase overexpression increases metastatic growth of B16 melanoma cells in the mouse liver. *Hepatology* **35**, 74–81.
44 Godwin AK, Meister A, O'Dwyer PJ, Huang CS, Hamilton TC & Anderson ME (1992) High resistance to cisplatin in human ovarian cancer cell lines is associated with marked increase of glutathione synthesis. *Proc Natl Acad Sci USA* **89**, 3070–3074.
45 Traverso N, Ricciarelli R, Nitti M, Marengo B, Furfaro AL, Pronzato MA, Marinari UM, Domenicotti C, Traverso N, Ricciarelli R *et al.* (2013) Role of glutathione in cancer progression and chemoresistance. *Oxid Med Cell Longev* **2013**, 972913.
46 Maclean KN, Janosík M, Kraus E, Kozich V, Allen RH, Raab BK & Kraus JP (2002) Cystathionine beta-synthase is coordinately regulated with proliferation through a redox-sensitive mechanism in cultured human cells and *Saccharomyces cerevisiae*. *J Cell Physiol* **192**, 81–92.
47 Macciò A & Madeddu C (2013) Cisplatin : an old drug with a newfound efficacy – from mechanisms of action to cytotoxicity. *Expert Opin Pharmacother* **14**, 1839–1857.
48 Tomiyama A, Serizawa S, Tachibana K, Sakurada K, Samejima H, Kuchino Y & Kitanaka C (2006) Critical role for mitochondrial oxidative phosphorylation in the activation of tumor suppressors Bax and Bak. *J Natl Cancer Inst* **98**, 1462–1473.
49 Wong JYY, Huggins GS, Debidda M, Munshi NC & De Vivo I (2008) Dichloroacetate induces apoptosis in endometrial cancer cells. *Gynecol Oncol* **109**, 394–402.
50 Perchiniak E, Lawrence SA, Kasten S, Woodard BA, Taylor SM & Moran RG (2007) Probing the mechanism of the hamster mitochondrial folate transporter by mutagenesis and homology modeling. *Biochemistry* **46**, 1557–1567.
51 Rao Z, Gao J, Zhang B, Yang B & Zhang J (2012) Cisplatin sensitivity and mechanisms of anti-HPV16 E6-ribozyme on cervical carcinoma CaSKi cell line. *Chinese-German J Clin Oncol* **11**, 237–242.
52 Van Tine BA, Kappes JC, Banerjee NS, Knops J, Lai L, Steenbergen RDM, Meijer CLJM, Snijders PJF, Chatis P, Broker TR *et al.* (2004) Clonal selection for transcriptionally active viral oncogenes during progression to cancer. *J Virol* **78**, 11172–11186.
53 Menga A, Iacobazzi V, Infantino V, Avantaggiati ML & Palmieri F (2015) The mitochondrial aspartate/glutamate carrier isoform 1 gene expression is regulated by CREB in neuronal cells. *Int J Biochem Cell Biol* **60**, 157–166.
54 Infantino V, Convertini P, Menga A & Iacobazzi V (2013) MEF2C exon α: role in gene activation and differentiation. *Gene* **531**, 355–362.
55 Abate C, Niso M, Infantino V, Menga A & Berardi F (2015) Elements in support of the "non-identity" of the PGRMC1 protein with the sigma2 receptor. *Eur J Pharmacol* **758**, 16–23.
56 Menga A, Infantino V, Iacobazzi F, Convertini P, Palmieri F & Iacobazzi V (2013) Insight into mechanism of in vitro insulin secretion increase induced

by antipsychotic clozapine: Role of FOXA1 and mitochondrial citrate carrier. *Eur Neuropsychopharmacol* **23**, 978–987.
57 Wang X-A, Xiang S-S, Li H-F, Wu X-S, Li M-L, Shu Y-J, Zhang F, Cao Y, Ye Y-Y, Bao R-F *et al*. (2014) Cordycepin induces S phase arrest and apoptosis in human gallbladder cancer cells. *Molecules* **19**, 11350–11365.
58 Infantino V, Iacobazzi V, Menga A, Avantaggiati ML & Palmieri F (2014) A key role of the mitochondrial citrate carrier (SLC25A1) in TNFα- and IFNγ-triggered inflammation. *Biochim Biophys Acta* **1839**, 1217–1225.
59 Kirchner T, Möller S, Klinger M, Solbach W, Laskay T & Behnen M (2012) The impact of various reactive oxygen species on the formation of neutrophil extracellular traps. *Mediators Inflamm* **2012**, 849136.
60 Palmieri EM, Spera I, Menga A, Infantino V, Porcelli V, Iacobazzi V, Pierri CL, Hooper DC, Palmieri F & Castegna A (2015) Acetylation of human mitochondrial citrate carrier modulates mitochondrial citrate/malate exchange activity to sustain NADPH production during macrophage activation. *Biochim Biophys Acta* **1847**, 729–738.
61 Vozza A, Parisi G, De Leonardis F, Lasorsa FM, Castegna A, Amorese D, Marmo R, Calcagnile VM, Palmieri L, Ricquier D *et al*. (2014) UCP2 transports C4 metabolites out of mitochondria, regulating glucose and glutamine oxidation. *Proc Natl Acad Sci USA* **111**, 960–965.
62 Palmieri EM, Menga A, Lebrun A, Hooper DC, Butterfield DA, Mazzone M & Castegna A (2016) Blockade of glutamine synthetase enhances inflammatory response in microglial cells. *Antioxid Redox Signal*, ars.2016.6715.
63 Castegna A, Scarcia P, Agrimi G, Palmieri L, Rottensteiner H, Spera I, Germinario L & Palmieri F (2010) Identification and functional characterization of a novel mitochondrial carrier for citrate and oxoglutarate in *Saccharomyces cerevisiae*. *J Biol Chem* **285**, 17359–17370.
64 Palmieri EM, Spera I, Menga A, Infantino V, Iacobazzi V & Castegna A (2014) Glutamine synthetase desensitizes differentiated adipocytes to proinflammatory stimuli by raising intracellular glutamine levels. *FEBS Lett* **588**, 4807–4814.
65 Infantino V, Iacobazzi V, Palmieri F & Menga A (2013) ATP-citrate lyase is essential for macrophage inflammatory response. *Biochem Biophys Res Commun* **440**, 105–111.
66 Baccarelli AA & Byun H-M (2015) Platelet mitochondrial DNA methylation: a potential new marker of cardiovascular disease. *Clin Epigenetics* **7**, 44.
67 Byun H-M & Barrow TM (2015) Analysis of pollutant-induced changes in mitochondrial DNA methylation. *Methods Mol Biol* **1265**, 271–283.
68 Song L, James SR, Kazim L & Karpf AR (2005) Specific method for the determination of genomic DNA methylation by liquid chromatography-electrospray ionization tandem mass spectrometry. *Anal Chem* **77**, 504–510.
69 Castegna A, Palmieri L, Spera I, Porcelli V, Palmieri F, Fabis-Pedrini MJ, Kean RB, Barkhouse DA, Curtis MT & Hooper DC (2011) Oxidative stress and reduced glutamine synthetase activity in the absence of inflammation in the cortex of mice with experimental allergic encephalomyelitis. *Neuroscience* **185**, 97–105.